International Conference on Space Optics—ICSO 2020

Virtual Conference

30 March–2 April 2021

Edited by Bruno Cugny, Zoran Sodnik, and Nikos Karafolas

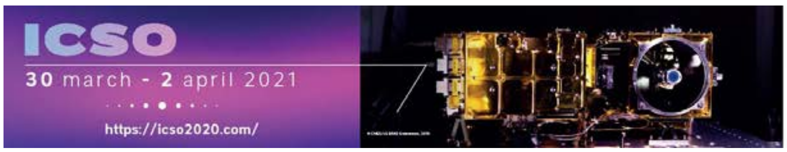

ICSO 2020
INTERNATIONAL CONFERENCE ON SPACE OPTICS
VIRTUAL

UV bandpass filters based on Ta_2O_5 and ZrO_2 for solar observation

esa icso proceedings cnes

International Conference on Space Optics — ICSO 2020, edited by Bruno Cugny, Zoran Sodnik, Nikos Karafolas, Proc. of SPIE Vol. 11852, 118521P · © 2021 ESA and CNES
CCC code: 0277-786X/21/$21 · doi: 10.1117/12.2599291

UV bandpass filters based on Ta_2O_5 and ZrO_2 for solar observation

Stefan Bruns[a]* (Stefan.bruns@ist.fraunhofer.de), Chris Britze[a] (chris.britze@ist.fraunhofer.de), Michael Vergöhl[a] (michael.vergoehl@ist.fraunhofer.de), Alex Feller[b] (feller@mps.mpg.de), Stefan Meining[b] (meining@mps.mpg.de)
[a]Fraunhofer Institute for Surface Engineering and Thin Films, Bienroder Weg 54E, 38100 Braunschweig, Germany;
[b]Max Planck Institute for Solar System Research, Justus-von-Liebig-Weg 3, 37077 Göttingen, Germany

ABSTRACT

In the present article, complex optical UV bandpass filters with tantalum pentoxide and zirconium dioxide as high refractive index materials, respectively, have been manufactured on the EOSS® sputtering system. Four different bandpass filters with central wavelengths between 316 nm and 399 nm and a blocking up to 1100 nm were realized. Transmittance of the filters was higher than 80% although the band pass was located close to the absorption edge of the high index material. For two of the filters, ZrO_2 was used as the high index material. It is demonstrated that the ZrO_2 containing filters have very good optical properties and ZrO_2 is a good alternative to the use of the costly HfO_2.

The bandpass filters will be used as order-sorting filters for the grating spectrograph of the Sunrise UV Spectropolarimeter and Imager (SUSI) onboard the balloon-borne solar observatory Sunrise III. The filters are designed to filter out unwanted light that hits the detectors. The observatory will be launched in June 2022. Among other topics, the mission is dedicated to the investigation of magnetic fields and convective plasma flows in the lower solar atmosphere.

Keywords: Magnetron Sputtering, Metamode, CARS, Broad band monitoring, Ultraviolet bandpass, Zirconium dioxide, Tantalum pentoxide

1. INTRODUCTION

Sunrise is a balloon-borne solar observatory dedicated to the investigation of key processes of the magnetic field and the plasma flows in the lower solar atmosphere. After two successful missions in 2009 and 2013 the third science flight of Sunrise is planned for June 2022. Sunrise III will carry dedicated instruments that will spectro-polarimetrically sample the photosphere and chromosphere in a multitude of spectral lines over a broad wavelength range from the near ultraviolet (309 nm) up to the near infrared (860 nm). The Max Planck Institute for Solar System Research is working on the Sunrise UV Spectropolarimeter and Imager (SUSI) that will explore the wavelength range from 309 nm to 417 nm at high spatial resolution and increased polarimetric sensitivity. This makes a lot of information available for scientific questions that was not available up to now. This wavelength range cannot be explored with high resolution and good signal-to noise ratio from ground because of the extinction of the UV light in the Earth atmosphere. Thus, the observatory will work in the stratosphere at an altitude of around 37 km. For further details see [1].

Four different bandpass filters at wavelengths 316 nm, 327 nm, 355 nm and 399 nm were needed for the SUSI as order-sorting filters. While those at 355 nm and 399 nm can be fabricated with well-established tantalum pentoxide [2], the other two filters have to be coated with another material that has a lower absorption in this wavelength range. Besides the absorption in the UV spectral region, scattering is often a typical issue, especially when ZrO_2 is used. Hafnium dioxide is often used as high refractive index material because of good optical properties in particular for laser coatings [3]. An alternative with a several times lower raw material price is zirconium dioxide. Both materials have the tendency to build up crystallinity during magnetron sputtering process. For low loss applications this must be suppressed. One way to do this is the addition of glass building materials like for example silicon dioxide. This can also lower the intrinsic stress of the films [4][5].

*stefan.bruns@ist.fraunhofer.de; phone +49 531 2155 628; fax +49 531 2155 900; www.ist.fraunhofer.de

2. EXPERIMENTAL

The coatings were performed on the Enhanced Optical Sputtering System (EOSS®), which is based on a turntable geometry [6][7][8]. For each material two double magnetron sources with cylindrical sputtering targets were used in compartments with high gas separation. An RF plasma source was used for post-oxidation, which required a rapid rotation of the turntable that holds the substrate carriers. The silicon target was made from crystalline tube parts. It was used for the low refractive index material SiO_2 in a Metamode process. This means that no additional oxygen was induced in the sputtering zone. The targets for the high refractive index materials ZrO_2 and Ta_2O_5 are based on zirconium-oxide and tantalum-oxide and were plasma-sprayed. The conductivity is arranged in such a way that mid frequency sputtering is possible. We call this compound assisted reactive sputtering (CARS). All targets were from high purity raw material. The cylindrical targets offer a large amount of material. The deposition rate virtually does not change overall the target lifetime because there are no racetrack trenches. This makes it possible to realize time-controlled layers or co-sputtering with extremely stable ratios [2][9][10].

Together with a target supplier we developed a sprayed target based on zirconium-oxide. It contains an amount of yttrium and aluminum also and has together with hafnium a purity better than 99.5%. For comparison, absorption results from different targets are plotted in Figure 1. Actually, these are the total losses that are calculated from the transmittance measurement of 2 µm thick layers in comparison with the uncoated fused silica substrate. The black curve represents a coating deposited with a metallic target made of standard Material ZR702 sputtered in Metamode. This material has a purity of 99.2 %. Even the addition of quite a lot of silicon did not help to get as low losses as needed for 80% transmittance in the bandpass filters at around 300 nm. Another sprayed target without focus on low impurities had even worse values as can be seen in the red line. The high purity target together with the addition of a few percent silicon by co-sputtering suppresses the crystallization and reduces straylight losses of the layers. The power ratio was 1:33, so the amount of silicon in the layer is very low and the refractive index is still high. This gives the low total losses of the green line which is the process we used. At 300 nm we have about 0.0003 and above 360 nm the value is below 0.0001 which is nearly the detection limit of this method. With a similar deposition rate of 0.21 nm/s but no silicon addition there is a huge effect from crystallinity which was determined by x-ray diffraction and can be seen in the blue curve.

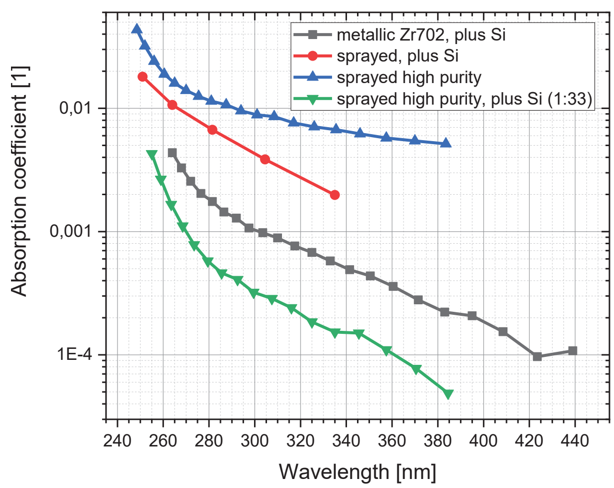

Figure 1. Absorption values from different targets and process types for 2 µm thick zirconia layers in the UV spectral range.

The refractive index was initially determined using ellipsometry from single layers. This was used for the first coating of a complete bandpass including the blocker. Afterwards the dispersion was fine-tuned from the final transmittance measurements of all layers using OptiRe. Doing this, we got a dispersion that describes all layer thicknesses from thin to thick. After this remodeling the refractive index was 2.09 at 550 nm. Figure 2 shows the final dispersion of the selected process in UV spectral range.

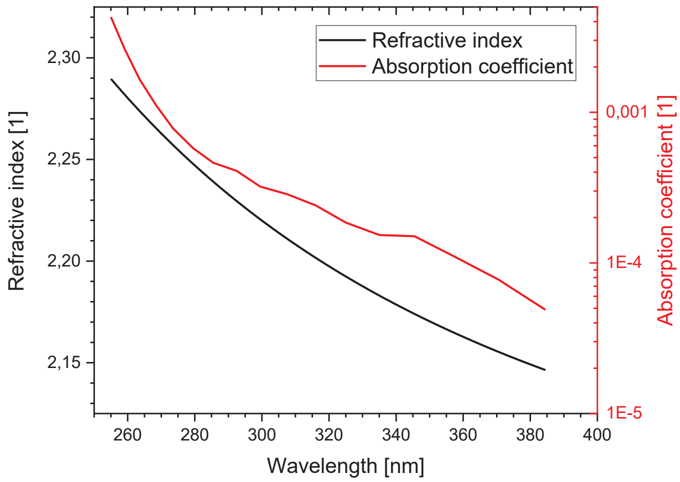

Figure 2. Refractive index and absorption coefficient that was used for the zirconium dioxide layers.

The substrates for the bandpass filters were made of UV fused silica and had a size of (40x40) mm with a thickness of 8 mm. The coating must have an aperture of at least 38 mm. For this reason, the substrates were fixed only on the edges during the deposition as the system is in the sputter-up configuration. Besides P4 polishing the surface figure requirement was below 65 nm.

The angle of incidence for the filters in the final installation is 2° as the substrates are mounted in tilted position. This makes it essential to do the design of the layer stack for bandpass and blocker on the same side of the substrate. Otherwise multiple back-reflections could occur resulting in ghost images. It is well known that the deposition of bandpass and blocker on the same side of a substrate is much more difficult because the bandpass stack interferes with the blocker stack. The optical design of the layers stacks was made using Optilayer. At first a bandpass based on three cavities in a quarter wave thickness design was calculated. Then the blocker was designed by gradual evolution with an antireflection range around the bandpass wavelength. Finally, the stacks were put together with most of the layers fixed. Only four layers at the connection were used for adjustment. A blocking of up to OD5 was needed within a range from 200 to 1100 nm. For this, layer thicknesses of more than 20 µm and layer numbers greater than 200 were necessary. The thickness and layer numbers are given in Table 1. For the bandpasses at 355 nm and 399 nm tantala was used as high refractive index material. The high index material for 316 nm and 327 nm was zirconia.

This increased the effort for the optical monitoring, which was performed by the broadband transmittance monitoring system MOCCA$^{+®}$. The control of the process was done on a separate test glass. Intermediate exchanges of the test glass for the broadband monitoring were needed to keep the bandpass smooth. Five substrates were used for the bandpass at 316 nm and four substrates for all other filters. With the first monitoring glass the bandpass filter consisting of QWOT layers and some layers of the blocker were applied.

Table 1. Thickness and number of layers of the filters according to their central wavelength and FWHM.

	BP316	**BP327**	**BP355**	**BP399**
Material	ZrO_2	ZrO_2	Ta_2O_5	Ta_2O_5
FWHM	18	20	24	32
Total thickness	21,6 µm	21,3 µm	21,3 µm	23,4 µm
Layers	252	230	216	226

On the backside a four-layer antireflective coating plus stress compensation layer were applied. The back reflection in the passband wavelength region was kept below 0.2 %.

MOCCA+® is not only a broad-band monitor, but it is able to control and simulate the complete production process. We defined the coating steps in material recipes inside the database of MOCCA+®. In this part we also defined the batch with details on machine preparation and the stack of single layers including the position of the monitoring glass exchange. The monitoring routine was selected by the help of the internal pre-calculation. For the in situ transmittance measurement a spectrometer system with a high long-term stability was used. The wavelength range was 380 nm to 1650 nm. A stable halogen lamp was the light source and the light path was designed robust with reflective collimators and fibers. Measurements were available for every turntable rotation. In our case at 250 rounds per minute, this means every 240 ms. All three parts of the transmittance measurement, including reference, dark and sample were collected during each rotation. The integration time was 2.7 ms. This means that we got the thickness evolution in very small steps.

The ex situ transmittance measurements were conducted with a Perkin Elmer Lambda 950 UV-VIS-NIR spectrophotometer and the standard transmittance accessory.

3. RESULTS

First tests with only the QWOT layers from bandpasses at 355 nm and 316 nm are shown Figure 3 as red curve compared to the initial design in black. The mismatch from design is only a slight shift to higher wavelength. We measured this in detail for the tantala based bandpass with 20 layers at 355 nm in the left graph. On the left side we measured 0.57 nm which means a plus of 0.17% and on the right we measured 0.73 nm which means a plus of 0.20%. Also, for the process with zirconia that was used for 316 nm nearly perfect match could be realized using the broad band monitoring as shown in the right graph. The wavelength range for the transmittance measurement was from 380 nm to 1650 nm and thus we had to use an extrapolated dispersion and monitoring out of the band. Even this had only a small effect on the bandpass position and shape.

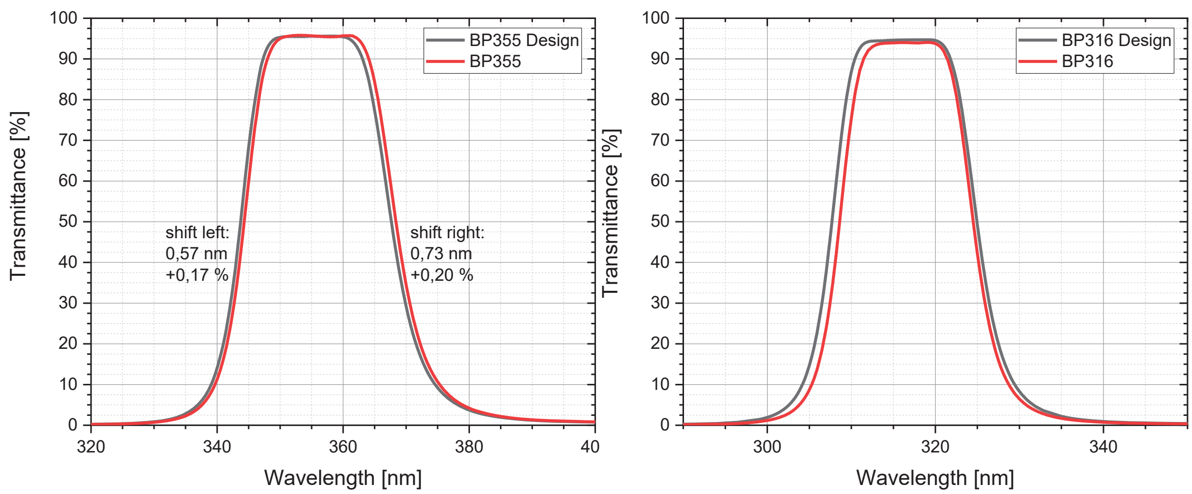

Figure 3. Transmittance measurement versus design for examples of the bandpass part of the layer stacks. Tantala based at central wavelength of 355 nm (left) and zirconia based at 316 nm (right).

The shape of the bandpass stayed in good match even for the complete coating with more than 200 layers. As an example, the bandpasses at 316 nm and 327 nm with 252 and 230 layers respectively are plotted in the graph of Figure 4. The measurements were done at samples that also got the backside coating for antireflection and stress compensation. For the 316 nm coating (blue curve) the absorption was slightly underestimated during the design (black curve). Annealing of the filters at 400°C in atmosphere brought the transmittance over the minimum target value of 80 % (red line). No wavelength shift could be seen. For the 327 nm filter no annealing was used. The transmittance of this filter is in expectable line with the as-deposited filter at 316 nm.

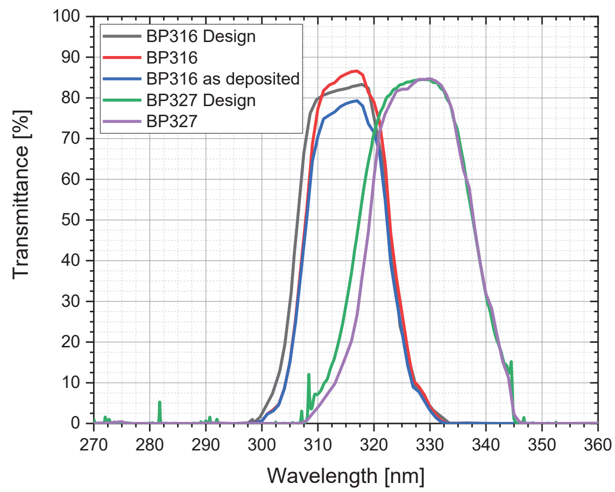

Figure 4. Transmittance from measurement compared with design for the zirconia based bandpass filters at 316 nm and 327 nm. Only the 316 nm sample was annealed which led to higher transmittance (from as deposited in blue to red after annealing).

The broad blocking range of the filters in terms of optical density is plotted in Figure 5. It is defined from 200 nm to 1100 nm. The graph shows one of the tantala filters in black and one of the zirconia filters in red. The overall optical density was better than OD3. At special wavelengths, the density must be OD5. This was close to the bandpass and in several wavelength ranges containing prominent solar spectral blend lines to be suppressed. Because of the slightly lower refractive index contrast and smaller full width half maximum the bandpass at 316 nm needed some more layers than that at 399 nm although the optical density is lower in the visible range.

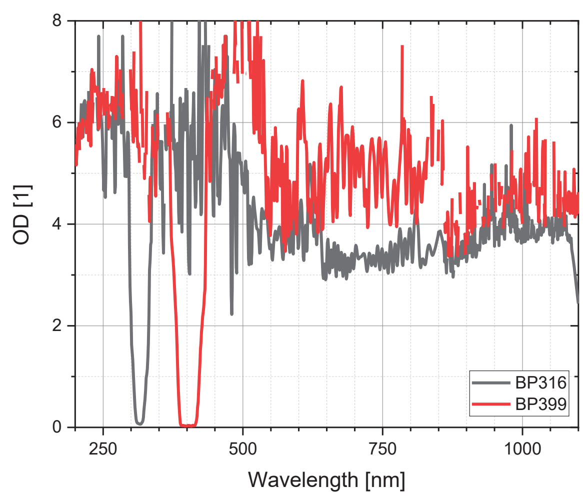

Figure 5 Optical density plot of one zirconia (316 nm) and one tantala (399 nm) based bandpass filter.

As an example of the coating errors from the single layers Figure 6 shows results from the MOCCA$^{+®}$ monitoring. The values are from a bandpass at 399 nm with four monitoring substrates. The monitoring glass was exchanged after layers 48, 92 and 146 (plotted as blue lines). After each layer a final thickness measurement was made and the resulting deposition rate was calculated from the coating time of that layer. At the beginning the machine was brought to the temperature region where it saturates in the process. Thus, we do not see any changes at the batch start. Also, the exchange of the substrates without additional heating phase does not lead to a different detected deposition rate. It remains very constant throughout the whole process. The average deposition rate over all layers was 0.32 nm/s for tantalum pentoxide and 0.26 nm/s for silicon dioxide. The deviations from target thickness are on a very low level, which confirms exact layer termination by the closing shutters. It has to be taken into consideration that no synchronization between shutter and turntable was made during this process. The mean error is lower for tantala with 0.001 nm (values from -0.63 nm to 0.22 nm) than for silica with 0.047 nm (values from -0.74 nm to 0.58 nm). The slight increase in spreading at the end can be connected to the relatively high layer count and total thickness that was monitored on the last glass. These were 80 layers in total.

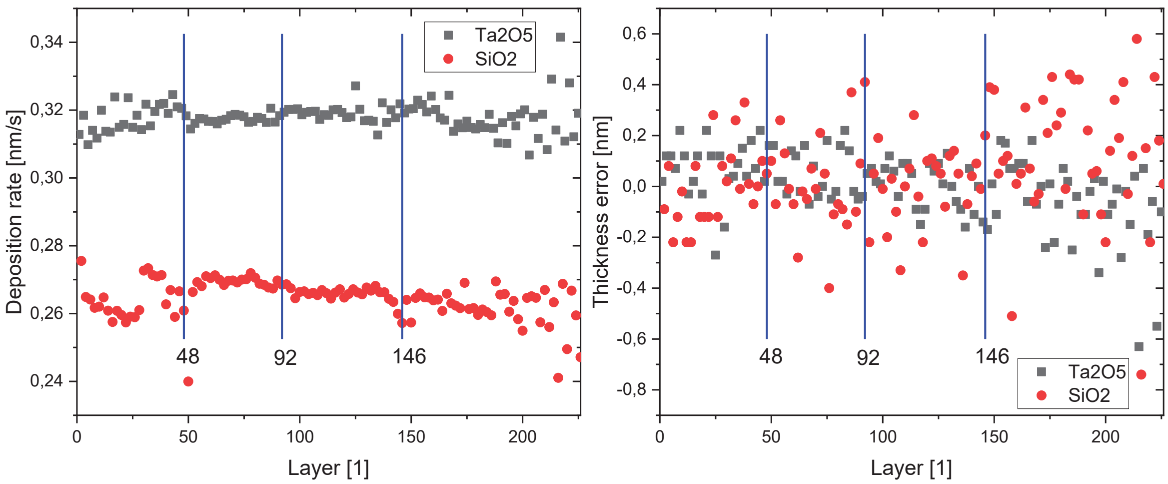

Figure 6. Calculated values for all layers of a full 399 nm bandpass stack from the MOCCA$^{+®}$ system. Left: Depositon rate from final measurement thickness divided by the coating time; Right: Thickness error as difference from target thickness.

Table 2. Measured compressive stress values for the filter coating and thickness of compensation layer on the backside.

	BP316	**BP327**	**BP355**	**BP399**
Stress	-54/-75 MPa	-58/-74 MPa	-91/-108 MPa	-94/-109 MPa
Compensation	2 µm SiO_2	2 µm SiO_2	5 µm SiO_2	5 µm SiO_2

The coated glasses needed stress compensation to meet the surface figure requirements. This was done as a silicon dioxide layer below the antireflective coating on the backside. We measured the profile of two fused silica substrates with a thickness of 1 mm at a Dektak system over a range of 40 µm. Measurements of one sample with the bandpass coating at 316 nm are shown the graph in Figure 7. We measured from both sides and each of them twice. The measurements revealed to be very reproducible with this method. From the maximum height value, we calculated the stress for all coatings using the Stoney formula [11]. The compressive stress was in the range from 50 MPa to 80 MPa for the zirconia based filters and in the range of 90 MPa to 110 MPa for the tantala based ones (single values of the substrates in Table 2). We decided to not fully compensate the stress to minimize the losses and applied a 2 µm silicon dioxide layer for the zirconia filters and a 5 µm layer for the tantala filters.

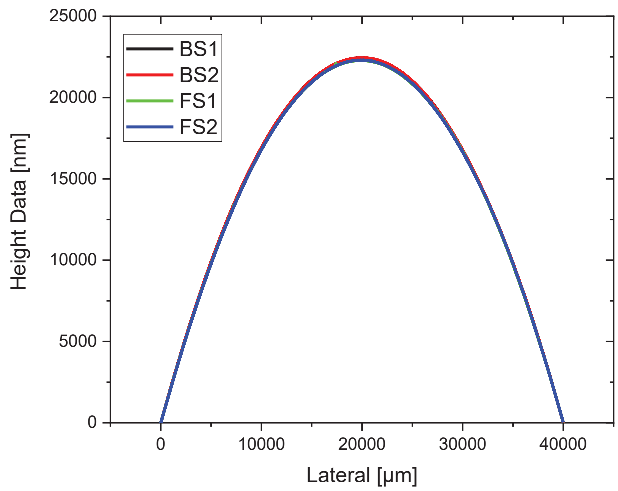

Figure 7. Shape measurement of an 1 mm thin fused silica substrate with a Dektak profilometer.

4. CONCLUSION

A cylindrical sputtering target from high grade zirconia was evaluated in an EOSS® coating machine. During the process development silicon dioxide was mixed into the layers. This led to good optical properties with losses of $3x10^{-4}$ at a wavelength of 300 nm and below $1x10^{-4}$ above 360 nm. The refractive index was modelled to 2.22 at 300 nm.

Four different bandpass filters in the wavelength range from 300 to 400 nm with a blocking from UV to 1100 nm were deposited. The calculated layer stacks consisted of more than 200 layers and thicknesses above 21 µm. On the backside the residual stress was compensated besides an antireflection coating.

The filters successfully passed a thermal-vacuum test inside their final holder. They are in the integration and verification phase inside the SUSI instrument for the SUNRISE III mission.

ACKNOWLEDGEMENT

The work was funded by the German Federal Ministry of Education and Research (BMBF) within the project EPIC-Lens (FKZ 13N14583) and the Max Planck Institute for Solar System Research within the project Sunrise III.

REFERENCES

[1] Feller, A., Gandorfer, A., Iglesias, F. A., Lagg, A., Riethmüller, T. L., Solanki, S. K., Katsukawa, Y., Kubo, M., "The SUNRISE UV Spectropolarimeter and Imager for SUNRISE III," Proc. SPIE 11447, Ground-based and Airborne Instrumentation for Astronomy VIII, 11447AK (2020); https://doi.org/10.1117/12.2562666.

[2] Vergöhl, M., Bruns, S., Rademacher, D. and Bräuer, G., "Industrial-scale deposition of highly uniform and precise optical interference filters by the use of an improved cylindrical magnetron sputtering system," Surf. Coat. Technol. 267, 53-58 (2015).

[3] Gallais, L., Capoulade, J., Natoli, J. Y., Commandré, M., Cathelinaud, M., Koc, C. and Lequime, M., "Laser damage resistance of hafnia thin films deposited by electron beam deposition, reactive low voltrage ion plating, and dual ion beam sputtering," Applied Optics 47(13), C107-C113 (2008).
[4] Pond, B. J., DeBar, J. I., Carniglia, C. K. and Raj, T., "Stress reduction in ion beam sputtered mixed oxide films," Appl. Opt. 28, 2080 (1989).
[5] Bruns, S., Vergöhl, M., "Optical and thin film properties of mixed oxides deposited by pulsed reactive magnetron sputtering," Proc. SPIE 8168, Advances in Optical Thin Films IV, 81680N (2011); https://doi.org/10.1117/12.896838.
[6] Rademacher, D., Bräuer, G., Vergöhl, M., Fritz, B., Zickenrott, T., "New sputtering concept for optical precision coatings," Proc. SPIE 8168, Advances in Optical Thin Films IV, 81680O (2011); https://doi.org/10.1117/12.896843.
[7] Rademacher, D., Zickenrott, T. and Vergöhl, M., “Sputtering of dielectric single layers by metallic mode reactive sputtering and conventional reactive sputtering from cylindrical cathodes in a sputter-up configuration," Thin Solid Films 532, 98-105 (2013).
[8] Vergöhl, M., Rademacher, D. and Pflug, A., "Progress on optical coatings deposited with dual rotatable magnetrons in a sputter up system," Surf. Coat. Technol. 241, 38-44 (2014).
[9] Bruns, S., Vergöhl, M., Zickenrott, Z., "Recent developments in precision optical coatings prepared by cylindrical magnetron sputtering," Proc. SPIE 9627, Optical Systems Design 2015: Advances in Optical Thin Films V, 96270N (2015); https://doi.org/10.1117/12.2191351.
[10] Rademacher, D., Bräuer, G., Fritz, B., Vergöhl, M. "Optical properties of silicon titanium oxide mixtures prepared by metallic mode reactive sputtering," Appl. Opt. 51, 8047-8051 (2012)
[11] Ohring, M., Materials Science of Thin Films. Academic Press, 2nd edition, 2002.